Resonant Capture in a System of Two Coupled Homoclinic Oscillators

R. H. RAND
D. D. QUINN
Cornell University, Department of Theoretical and Applied Mechanics, Cornell University, Ithaca, NY 14853, U. S. A.

Abstract: The authors investigate the dynamics of a system of two coupled oscillators, each of which has a separatrix loop in its uncoupled phase portrait. The effect of the coupling, which is of the diffusive viscous type, is to enhance the region C_ε of phase space, which consists of all motions that do not escape to infinity. The authors offer numerically obtained descriptions of the region C_ε, as well as some analytical investigations into its location and nature.

Key Words: Coupled oscillators, capture, homoclinic, separatrix

INTRODUCTION

In this article, we investigate some of the dynamics of the following system of coupled oscillators:

$$\ddot{x}_1 - \frac{1}{2}x_1^2 - x_1 = \varepsilon(\dot{x}_2 - \dot{x}_1), \qquad \ddot{x}_2 - \frac{1}{2}x_2^2 - x_2 = \varepsilon(\dot{x}_1 - \dot{x}_2). \tag{1}$$

This system is related to a system of two coupled pendulums (see appendix). When the coupling constant ε is taken equal to zero, we have two identical homoclinic oscillators. Each of these oscillators possesses a *homoclinic orbit* (also known as a separatrix or saddle connection; see Figure 1). The coupling terms in system (1) may be described as diffusive viscous coupling.

Our interest in the system (1) stems from two sources. First, it is an extension of other systems of two coupled oscillators that have already been studied. For example, a system consisting of two coupled Duffing oscillators was studied by Kauderer (1958) and by Rosenberg (1966) and his associates. The key phenomenon for such a system is the appearance of *nonlinear normal modes*. As another example, take a system of two coupled van der Pol oscillators, which was studied by Rand and Holmes (1980) and their associates. In this case, the key phenomenon is *phase locking* (or phase entrainment) versus drift. In the case of equation (1), the key phenomenon is *resonant capture* versus escape to infinity. This brings us to the second source of interest in system (1) because the phenomenon of resonant capture has recently been the focus of a number of articles involving single oscillators driven by slowly varying feedback. For example, Rand, Kinsey, and Mingori (1992) studied the system

$$\ddot{x} - x^2 = -w, \quad \dot{w} = \varepsilon, \tag{2}$$

Journal of Vibration and Control **1**: 41-56, 1995

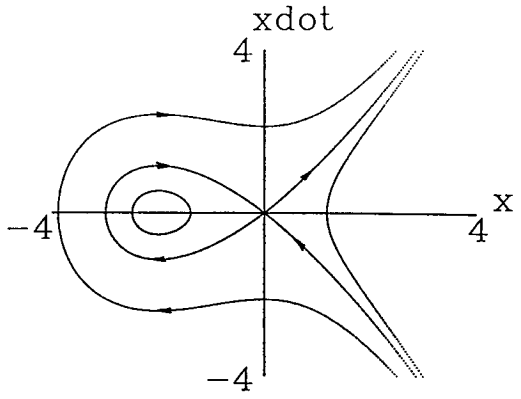

Figure 1. Phase portrait for a homoclinic oscillator, $\ddot{x} - \frac{1}{2}x^2 - x = 0$. The point (−2,0) is a center and the origin is a saddle. The separatrix loop intersects the x axis at $x = -3$ (and at the origin). It is thickest at $x = -2$, where $\dot{x} \cong \pm 1.15$.

whereas Quinn, Rand, and Bridge (1995) studied the system

$$\ddot{x} - x^2 = -w\left[1 - \frac{1}{2}x^2\right], \quad \dot{w} = \varepsilon\left[1 - \frac{1}{2}x^2\right] \tag{3}$$

Both systems (2) and (3) share with (1) the presence of a homoclinic orbit when $\varepsilon = 0$. All three systems exhibit resonant capture, which may be described by imagining that the separatrix of the $\varepsilon = 0$ system persists as an *instantaneous separatrix* in the perturbed system. As time goes on, the instantaneous separatrix changes its position, and motions that pass near it may cross it and become captured. Another way of looking at this phenomenon is to note that the saddle connection in the $\varepsilon = 0$ system is *structurally unstable* and that it may be expected to break under the various perturbations, thereby permitting motions that began outside the separated region in the $\varepsilon = 0$ system to enter inside that region when $\varepsilon > 0$.

In this article, we first describe the dynamics of system (1) as obtained by numerical integration. Then we offer some analysis of system (1) in an attempt to explain the numerical results.

RESONANT CAPTURE

A given initial condition $(x_1(0), \dot{x}_1(0), x_2(0), \dot{x}_2(0))$ to equations (1) will lead to a motion that either remains "captured" in the phase plane for all t or "escapes" to infinity in finite time. To illustrate these two situations, we numerically integrate equations (1) with $\varepsilon = 0.1$ for the following two sets of initial conditions:

$$x_1(0) = 1.29, \dot{x}_1(0) = -2, x_2(0) = -2, \dot{x}_2(0) = 0 \text{ escapes (Figure 2)}$$

$$x_1(0) = 1.31, \dot{x}_1(0) = -2, x_2(0) = -2, \dot{x}_2(0) = 0 \text{ captured (Figure 3).}$$

Figures 2 and 3 display the $x_1 - \dot{x}_1$ and $x_2 - \dot{x}_2$ phase planes for each of these initial conditions.

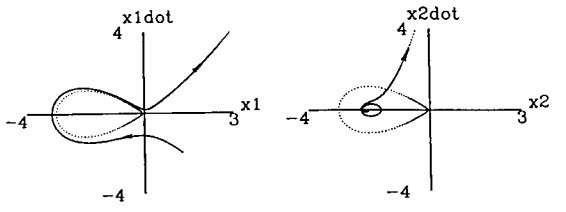

Figure 2. Sample numerical integration of equations (1) with $\varepsilon = 0.1$ for an initial condition that leads to escape. $x_1(0) = 1.29$, $\dot{x}_1(0) = -2$, $x_2(0) = -2$, $\dot{x}_2(0) = 0$. The separatrix of the $\varepsilon = 0$ problem is shown dotted.

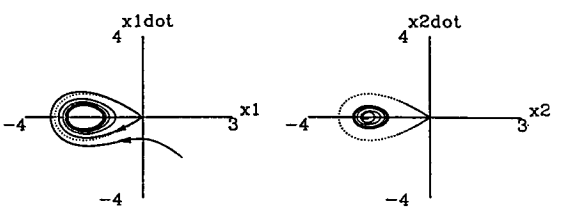

Figure 3. Sample numerical integration of equations (1) with $\varepsilon = 0.1$ for an initial condition that leads to capture. $x_1(0) = 1.31$, $\dot{x}_1(0) = -2$, $x_2(0) = -2$, $\dot{x}_2(0) = 0$. The separatrix of the $\varepsilon = 0$ problem is shown dotted.

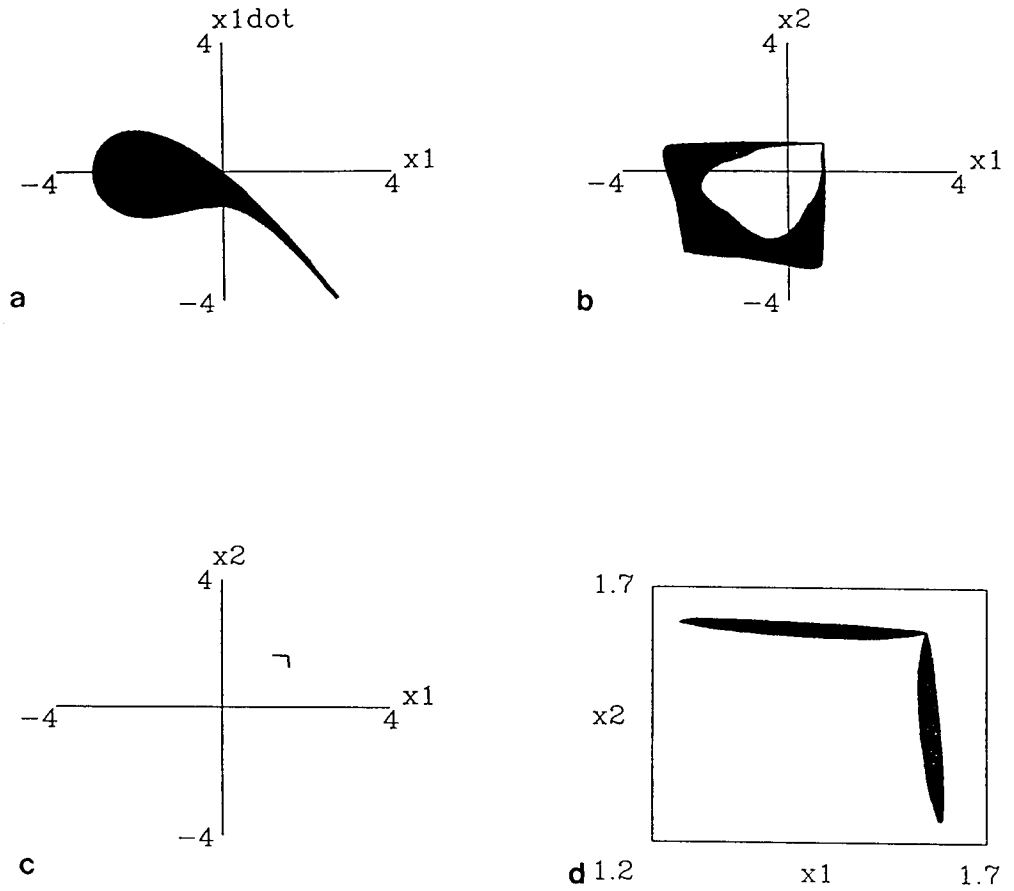

Figure 4. Some two-dimensional slices of the four-dimensional capture region C_ε for $\varepsilon = 0.1$. In each case, two initial conditions are fixed and two are varied. The darkened areas are initial conditions that lead to capture. (a) $x_2(0) = -2$, $\dot{x}_1(0) = 0$; (b) $\dot{x}_1(0) = -1$, $\dot{x}_2(0) = -1$; (c) $\dot{x}_1(0) = -2$, $\dot{x}_2(0) = -2$; (d) a magnification of panel c.

The question that interests us is, which initial conditions lead to capture and which lead to escape? For a given ε, let C_ε represent that region of the $\mathbb{R}^4$ phase space that leads to capture. Because C_ε is four dimensional, it is difficult for us to imagine and to illustrate. To do so, we may take "slices" of it by fixing two of the initial conditions and varying two. Figure 4 offers some glimpses at C_ε for $\varepsilon = 0.1$ and for three different slices through $\mathbb{R}^4$. By contrast, Figure 5 displays slices through the initial condition $\dot{x}_1(0) = -0.5$, $\dot{x}_2(0) = -1.5$ for three different values of ε.

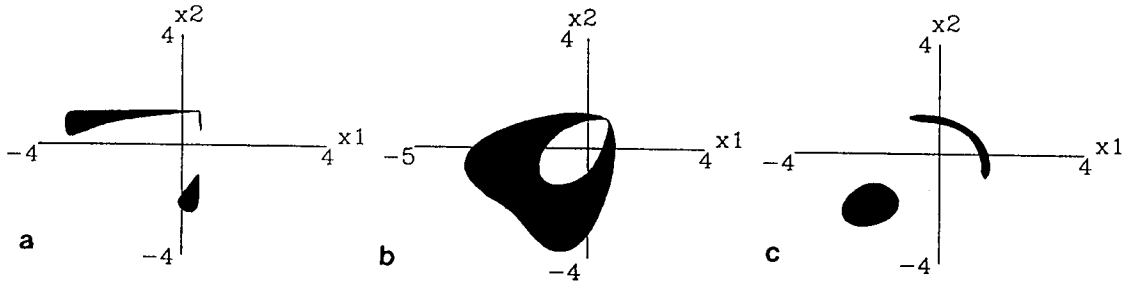

Figure 5. Three slices through C_ε for different values of ε. All correspond to the fixed initial conditions $\dot{x}_1(0) = -0.5$, $\dot{x}_2(0) = -1.5$. (a) $\varepsilon = 0.1$; (b) $\varepsilon = 1$; (c) $\varepsilon = 20$. The darkened areas are initial conditions that lead to capture.

The rest of this article is aimed at trying to understand the structure of C_ε by examining the dynamics of system (1).

BASIC CONSIDERATIONS

We begin by considering the individual uncoupled oscillators in (1):

$$\ddot{x} - \frac{1}{2}x^2 - x = 0. \tag{4}$$

Equation (4) has two equilibria, a saddle at the origin and a center at $x = -2$ (see Figure 1). Energy is conserved in the form

$$\frac{1}{2}\dot{x}^2 - \frac{1}{6}x^3 - \frac{1}{2}x^2 = h = \text{constant}. \tag{5}$$

The separatrix loop corresponds to $h = 0$. It intersects the x axis at $x = -3$ and at the origin. The separatrix achieves its maximum thickness at $x = -2$, at which point $\dot{x} = \pm 2/\sqrt{3} \cong \pm 1.15$. Points in the $x - \dot{x}$ phase plane that lie interior to the separatrix loop correspond to $h < 0$, whereas points outside the separatrix loop correspond to both $h > 0$ and $h < 0$.

Next we note that because the uncoupled oscillators in (1) are identical and the coupling vanishes when $\dot{x}_1 = \dot{x}_2$, the system (1) has a special symmetry, the invariance of the plane $x_1 = x_2$. In the four-dimensional phase space $x_1 - \dot{x}_1 - x_2 - \dot{x}_2$ this becomes a two-dimensional plane P:

$$P = \{(x_1, \dot{x}_1, x_2, \dot{x}_2) \mid x_1 = x_2, \dot{x}_1 = \dot{x}_2\}. \tag{6}$$

Any motion starting in P remains there for all time. From uniqueness in the autonomous system (1), any motion that does not lie in P at $t = 0$ can never pass through P in finite time. Motion in the plane P involves no coupling and therefore has the phase portrait shown in Figure 1.

In contrast to the uncoupled oscillator (4), the coupled system (1) is not conservative. Information about the dissipation of energy may be obtained by multiplying (1.1) by $\dot{x}_1$ and multiplying (1.2) by $\dot{x}_2$, and adding, with the following result:

$$\frac{dH}{dt} = -\varepsilon (\dot{x}_1 - \dot{x}_2)^2 \tag{7}$$

where H is the energy associated with the two uncoupled oscillators:

$$H = \left[\frac{1}{2}\dot{x}_1^2 - \frac{1}{6}x_1^3 - \frac{1}{2}x_1^2\right] + \left[\frac{1}{2}\dot{x}_2^2 - \frac{1}{6}x_2^3 - \frac{1}{2}x_2^2\right]. \tag{8}$$

Equation (7) shows that the energy H is a nonincreasing function of time t. Because the right-hand side of equation (7) is not negative definite, however, we cannot conclude that H tends toward its minimum value. However, H must asymptotically approach some constant value h_0 for every motion that is bounded. Thus the right-hand side of (7) must go to zero for these captured motions, a condition that is satisfied only by motions that lie in the invariant plane P.

Thus every captured trajectory eventually approaches a periodic motion lying in the invariant plane P, a fact that is confirmed by numerical integration of the coupled system (1) (cf. Figure 3). Any such periodic motion $x_1 = x_2 = f(t)$ satisfies the differential equation

$$\ddot{f} - \frac{1}{2}f^2 - f = 0 \tag{9}$$

and is given by the analytical expression

$$x_1 = x_2 = f(t) = A + B\,\mathrm{sn}^2\,(u,m) \tag{10}$$

where

$$A = -1 - \frac{1+m}{\alpha^2}, \quad B = \frac{3m}{\alpha^2}, \quad \alpha^4 = 1 - m + m^2, \quad u = \frac{t - t_0}{2m} \tag{11}$$

and where $\mathrm{sn}(u,m)$ is the Jacobi elliptic function with square modulus m (Rand, 1994). Here $m = 0$ corresponds to the equilibrium $f(t) \equiv -2$, whereas $m = 1$ corresponds to motion on the separatrix, which may be written in the simplified form

$$x_1 = x_2 = f(t) = \frac{-3}{\cosh^2\left[\dfrac{t - t_0}{2}\right]}, \quad m = 1 \text{ (separatrix)}. \tag{12}$$

To investigate the *stability* of the periodic motions (10), we transform coordinates from $(x_1, \dot{x}_1, x_2, \dot{x}_2)$ to $(y_1, \dot{y}_1, y_2, \dot{y}_2)$:

$$y_1 = x_1 + x_2, \quad y_2 = x_1 - x_2. \tag{13}$$

Equations (1) become

$$\ddot{y}_1 - \frac{1}{4}y_1^2 - y_1 - \frac{1}{4}y_2^2 = 0, \quad \ddot{y}_2 - y_2\left[\frac{1}{2}y_1 + 1\right] = -2\varepsilon\dot{y}_2. \tag{14}$$

Linear stability of $x_1 = x_2 = f(t)$ may be determined by setting

$$y_1 = 2f(t) + \eta_1, \; y_2 = 0 + \eta_2 \tag{15}$$

in equation (14) and linearizing in η_1, η_2, giving the variational equations

$$\ddot{\eta}_1 - [1 + f(t)]\,\eta_1 = 0, \tag{16.1}$$

$$\ddot{\eta}_2 - [1 + f(t)]\,\eta_2 = -2\varepsilon\dot{\eta}_2. \tag{16.2}$$

Note that the invariant plane P, equation (6), when expressed in $y_1 - y_2$ coordinates, becomes $y_2 = 0$. This shows that equation (16.1) represents the effects of a small deviation within the invariant plane P, whereas (16.2) similarly governs the growth of deviations normal to P.

Equation (16.1) is a Hill's equation (Magnus and Winkler, 1966; Stoker, 1950). One of its linearly independent solutions is given by $\eta_1 = df/dt$, a periodic function. This follows at once by differentiating equation (9) for $f(t)$, which gives

$$\dddot{f} - [1 + f]\,\dot{f} = 0. \tag{17}$$

Thus one of the Floquet multipliers of equation (16.1) is unity. Because the product of the Floquet multipliers for a Hill's equation is unity (Stoker, 1950), we have that the second Floquet multiplier is also unity. The second independent solution of (16.1) grows linearly in t (see Stoker, 1950), reflecting the Lyapunov instability of periodic motions in the invariant plane P due to the dependence of their period on amplitude. These motions are, however, orbitally stable to deviations in the plane P.

Equation (16.2) may be treated by setting

$$\eta_2 = e^{-\varepsilon t}v \tag{18}$$

giving the following equation on v:

$$\ddot{v} - [\,1 + \varepsilon^2 + f(t)]\,v = 0. \tag{19}$$

For small ε, equation (19) is close to equation (16.1), which we just discussed. Thus, if we neglect terms of $O(\varepsilon^2)$ in (19), we see that solutions v grow no faster than linearly in t, and hence that all solutions η_2 are bounded, from (18). For large values of ε, we have investigated the stability of equation (16.2) by using numerical integration with Floquet theory. We found that (16.2) was stable for all values of m (cf. equation [11]) and ε.

Thus the region of the invariant plane P that lies inside the separatrix loop is attractive, although the individual periodic motions that fill it are only neutrally stable relative to deviations within the plane P. In addition, from the previous energy analysis (cf. equation [7]), every bounded motion approaches this invariant plane. Our stability analysis, however, gives us no information as to which motion a particular initial condition approaches.

Let us next consider the equilibria of the coupled system (1). The two equilibria of the uncoupled oscillator (4), namely $(x, \dot{x}) = (0, 0)$ and $(-2, 0)$, lead to four equilibria in the coupled system (1): $(x_1, \dot{x}_1, x_2, \dot{x}_2) = (0, 0, 0, 0)$, $(0, 0, -2, 0)$, $(-2, 0, 0, 0)$, and $(-2, , -2, 0)$. Linearization of equations (1) about each of these equilibria gives the following stability results:

Equilibrium	*Eigenvalues*	*Type*
(0, 0, 0, 0)	$\lambda_1 = 1, \lambda_2 = -1, \lambda_{3,4} = -\varepsilon \pm \sqrt{\varepsilon^2 + 1}$	saddle
(0, 0, –2, 0)	$\lambda_1 > 0, \lambda_2 < 0, \lambda_{3,4} = -\mu^2 \pm \omega i$	saddle-focus
(–2, 0, 0, 0)	same as (0, 0, –2, 0)	
(–2, 0, –2, 0)	$\lambda_1 = i, \lambda_2 = -i, \lambda_{3,4} = -\varepsilon \pm \sqrt{\varepsilon^2 - 1}$	focus-center ($\varepsilon < 1$) node-center ($\varepsilon \geq 1$)

In the case of (0, 0, –2, 0) and (–2, 0, 0, 0), μ and ω are abbreviations for complicated functions of ε.

THE CAPTURE REGION C_ε

It is easy to characterize the capture region C_ε for $\varepsilon = 0$ because in that case equations (1) become the Cartesian product of two copies of equation (4). Capture can occur in equation (4) only if motions start inside the separatrix loop or lie on the unbounded branch of the stable manifold (S manifold) of the saddle. The $\varepsilon = 0$ capture region C_0 thus has (i) a four-dimensional component consisting of points $(x_1, \dot{x}_1)$ and $(x_2, \dot{x}_2)$ that lie inside the respective saddle loops; (ii) a three-dimensional component if the $(x_1, \dot{x}_1)$ point lies inside the saddle loop while the $(x_2, \dot{x}_2)$ point lies on the unbounded branch of the S manifold of the saddle, or vice versa; and (iii) a two-dimensional component if both $(x_1, \dot{x}_1)$ and $(x_2, \dot{x}_2)$ lie on the unbounded branch of the S manifold (see Figure 6).

We may expect that for small enough $\varepsilon > 0$, C_ε looks similar to C_0, but that all of its components are four dimensional. This is confirmed by numerical integration. For example, Figure 4c with $\varepsilon = 0.1$ shows a four-dimensional C_ε that corresponds to the two-dimensional C_0 in Figure 6c.

Next, consider the form of the slice through C_ε corresponding to the initial conditions $x_2(0) = -2$, $\dot{x}_2(0) = 0$ (i.e., the second oscillator is initially at rest at its [uncoupled] equilibrium point; see Figure 4a). For small ε, we may expect that x_2 remains close to its equilibrium during the time that x_1 motions are being captured. This situation may be investigated analytically by perturbing off of the S manifold of the equilibrium $(x_1, \dot{x}_1, x_2, \dot{x}_2) = (0, 0, -2, 0)$. For $\varepsilon = 0$, this S manifold consists of the Cartesian product of the motion on the S manifold of the saddle at the origin in the $x_1 - \dot{x}_1$ plane with the stable equilibrium at $x_2 = -2$, $\dot{x}_2 = 0$. Note that there are two branches of the S manifold of the saddle at the origin here: the separatrix loop and the unbounded branch. For small $\varepsilon > 0$, we neglect terms of $O(\varepsilon^2)$ and set

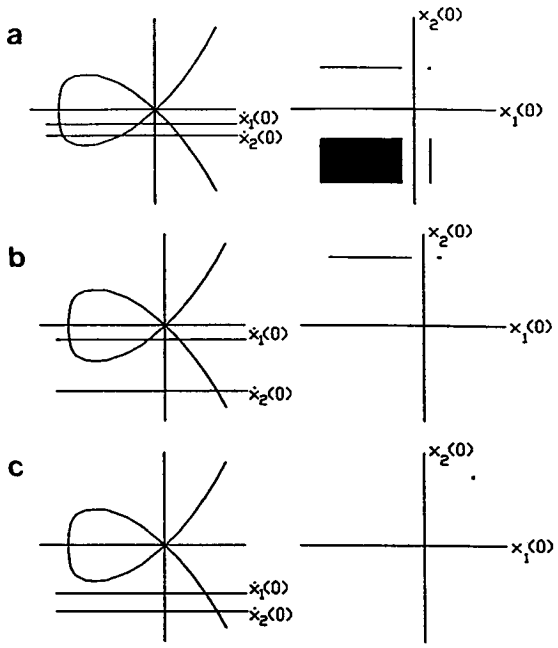

Figure 6. Behavior of the $\varepsilon = 0$ capture region C_0. In each case, the initial velocities $\dot{x}_1(0)$ and $\dot{x}_2(0)$ are fixed at values displayed on the phase plane shown at the left. The initial conditions $x_1(0)$ and $x_2(0)$ that lead to capture are shown on the right.

$$x_1 = g(t) + \varepsilon \xi_1 , \quad x_2 = -2 + \varepsilon \xi_2 \tag{20}$$

where $g(t) = \dfrac{-3}{\cosh^2\left[\dfrac{t - t_0}{2}\right]}$ for the motion around the unperturbed separatrix (cf. equation [12]) or

where $g(t) = \dfrac{3}{\sinh^2\left[\dfrac{t - t_0}{2}\right]}$ for the motion on the unbounded branch. These may both be treated

analytically at the same time by writing

$$g(t) = \frac{-12\, z}{e^{t - t_0} + e^{-(t - t_0)} + 2z} \tag{21}$$

where $z = +1$ corresponds to motion around the separatrix loop and $z = -1$ corresponds to motion on the unbounded branch of the S manifold of the saddle. Substituting (20) into (1) and neglecting terms of $O(\varepsilon^2)$ gives

$$\ddot{\xi}_1 - [1 + g]\, \xi_1 = -\dot{g}, \tag{22.1}$$

$$\ddot{\xi}_2 + \xi_2 = \dot{g}. \tag{22.2}$$

Because g and $\dot{g}$ are bounded functions that approach zero as t goes to infinity, the ξ_2 motion will remain bounded. Thus from (20), x_2 cannot leave the neighborhood of its initial position and its trajectory in the $x_2 - \dot{x}_2$ plane cannot represent a boundary between motions that escape and that remain captured. A trajectory that approaches the origin in the $x_1 - \dot{x}_1$ plane, on the other hand, will represent such a boundary. Here equation (22.1) on ξ_1 characterizes the breaking of the $\varepsilon = 0$ separatrix. Thus we may expect the trajectory that approaches the origin in the $x_1 - \dot{x}_2$ plane to approximate for small ε the boundary of C_ε, sliced by the plane $x_2(0) = -2$, $\dot{x}_2(0) = 0$ as in Figure 4a.

To solve equation (22.1), we use an approach due to Vakakis (1994) (see Rand, 1994; Quinn and Rand, 1994). First note that (22.1) possesses a complementary solution $\xi_1 = \dot{g}$, by the same reasoning as that used in equation (17) to show that (16.1) had the solution $\dot{f}$. Then we obtain a second independent complementary solution by using variation of parameters, $\xi_1 = u\,\dot{g}$, where u is to be found. Substituting into (22.1) gives $\dot{u} = 1/\dot{g}^2$, which may be integrated in closed form for g as in (21). For brevity, we omit the explicit form of the resulting complementary solution but write it instead as

$$\xi_{1\text{comp}} = c_1 F_1(t) + c_2 F_2(t). \tag{23}$$

Now to find a particular solution of (22.1), we again use variation of parameters, permitting c_1 and c_2 in (23) to depend on t. Again substituting into (22.1) gives the following equations on c_1 and c_2:

$$\dot{c}_1 = F_2\dot{g}, \qquad \dot{c}_2 = -F_1\dot{g} \tag{24}$$

where we have used the fact that the Wronskian $F_2\dot{F}_1 - F_1\dot{F}_2$ equals -1. Using MACSYMA to integrate equations (24), we obtain the following expression for a particular solution to equation (22.1):

$$\xi_{1\text{part}} = z\,e^{-\tau}\,\frac{((30\tau + 15)\,e^{3\tau} - (30\tau + 95)\,z\,e^{2\tau} + 15\,e^{\tau} + z)}{5(z + e^{\tau})^3} \tag{25}$$

where $\tau = t - t_0$ and where z is ± 1 depending on which branch of the S manifold is being considered.

Now it turns out that the complementary solution F_2 blows up as t goes to infinity, whereas $\xi_{1\text{part}}$ and F_1 remain bounded. So we must take $c_2 = 0$ in (23) for motions on the S manifold. Moreover, Vakakis (1994) has shown that the effect of c_1 is to time-shift the solution to order ε. Such a time shift does not alter the shape of the corresponding trajectory in the $x_1 - \dot{x}_1$ plane, and so we take $c_1 = 0$ for simplicity. Then the expression for x_1 on the S manifold becomes

$$x_1 = g(t) + \varepsilon\,\xi_{1\text{part}} + O(\varepsilon^2) \tag{26}$$

where $\xi_{1\text{part}}$ is given by equation (25). Equation (26) is displayed in Figure 7 for $\varepsilon = 0.1$. Comparison with Figure 4a shows reasonable agreement for large t.

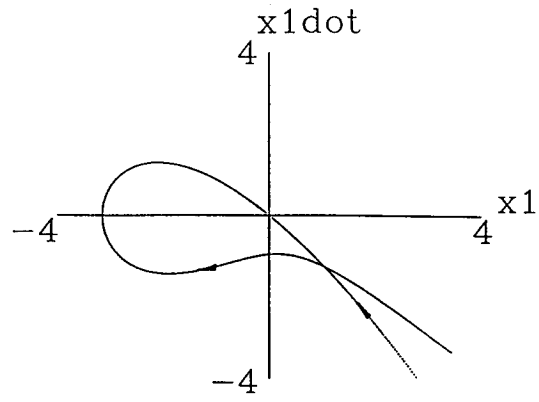

Figure 7. The perturbation approximation equation (26) for the S manifold of the equilibrium $x_1 = 0$, $x_2 = -2$ displayed in the $x_1 - \dot{x}_1$ plane. The tail of the component that wraps around the separatrix loop is inaccurate for $x_1 > 0$. As discussed in the text, this curve is expected to be close to the slice through C_ε corresponding to the initial conditions $x_2(0) = -2$, $\dot{x}_2(0) = 0$ (cf. Figure 4a).

The points in C_ε may be described as lying on the union of the S manifolds of all the periodic motions (10) in the invariant plane P. Because these periodic motions form a one-parameter family of orbits lying in the two-dimensional plane P, the S manifold of each one must be three dimensional because, when taken together, all these S manifolds must account for the four-dimensional region C_ε. On the other hand, the linear stability analysis of these periodic motions performed previously (cf. equations [16]) showed that there are only two dimensions that are locally attractive (i.e., the S manifold is locally two dimensional near the periodic motions in P). Evidently, a three-dimensional continuum of orbits must approach this two-dimensional set in order that the S manifold of an individual periodic motion be three dimensional.

STRUCTURE OF THE INTERIOR OF C_ε

We have seen that the fate of all motions that do not escape to infinity is to approach a periodic motion that lies inside the separatrix loop in the invariant plane P (cf. equation [6] and Figure 1). Greater understanding of the dynamics of system (1) may be obtained by investigating the structure of the interior of C_ε—that is, by associating an initial condition in C_ε with the periodic orbit that it approaches asymptotically. We characterize a periodic orbit in the invariant plane P by giving its energy h as defined by equation (5). The limiting cases are the equilibrium at $x = -2$, $\dot{x} = 0$, for which $h = -\frac{2}{3}$, and the separatrix, for which $h = 0$. Figure 8 shows the asymptotic value obtained numerically for h as a function of $x_1(0)$, as the latter is varied across the capture region for $\varepsilon = 0.1$ and for the initial conditions $\dot{x}_1(0) = -2$, $x_2(0) = -2$, $\dot{x}_2(0) = 0$.

Note the dependence of the asymptotic value of h on the initial condition in Figure 8. The effect is most pronounced near ∂C_ε, the boundary of the capture region, where we see an oscillatory dependence of h on $x_1(0)$. Small differences in initial condition are seen to lead to large differences in h.

To investigate this phenomenon analytically, we set up a perturbation scheme centered on the equilibrium $(x_1, \dot{x}_1, x_2, \dot{x}_2) = (-2, 0, -2, 0)$, which lies in the deep interior of the $\varepsilon = 0$ separatrix loops. We set

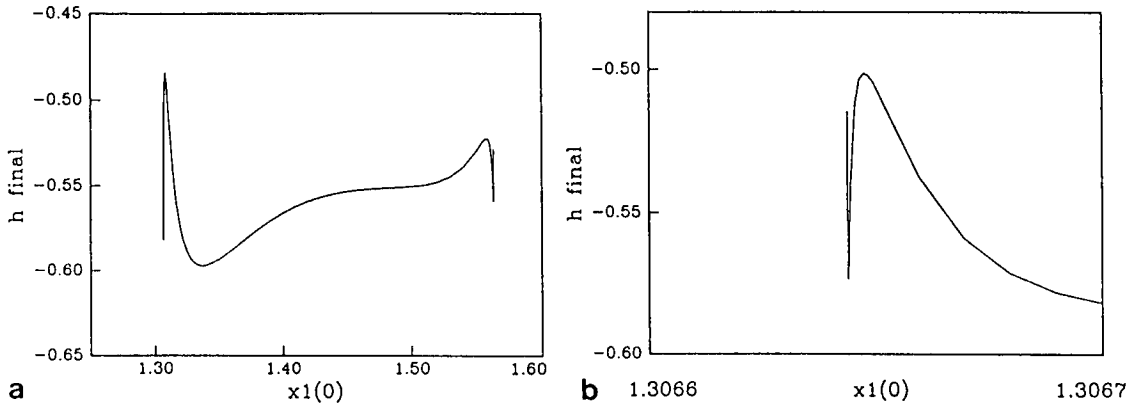

Figure 8. Panel a is the final energy h of equation (5) displayed as a function of the initial condition $x_1(0)$ for $\varepsilon = 0.1$ and for $\dot{x}_1(0) = -2$, $x_2(0) = -2$, $\dot{x}_2(0) = 0$. These values apply to Figure 4a, which see. Fix the vertical coordinate at $\dot{x}_1(0) = -2$ and imagine sweeping across the darkened region horizontally. Each initial condition so chosen ends up on some periodic motion for which $x_1(t) = x_2(t)$ and which lies inside the separatrix of Figure 1. Note that the dependence of h_{final} on $x_1(0)$ is very sensitive near ∂C_ε. Panel b is a magnification of the left edge of panel a.

$$x_i = -2 + \mu z_i, \qquad \mu << 1, \; i = 1, 2. \tag{27}$$

Substitution of (27) into (1) gives

$$\begin{aligned} \ddot{z}_1 + z_1 - \frac{1}{2}\mu z_1^2 &= \varepsilon (\dot{z}_2 - \dot{z}_1), \\ \ddot{z}_2 + z_2 - \frac{1}{2}\mu z_2^2 &= \varepsilon (\dot{z}_1 - \dot{z}_2). \end{aligned} \tag{28}$$

Because the quadratic terms will not produce secular terms in a perturbation method until $O(\mu^2)$ terms (see, e.g., Rand and Armbruster, 1987, pp. 10-13), it is natural to set $\varepsilon = \mu^2$ in (28), giving

$$\ddot{z}_1 + z_1 - \frac{1}{2}\mu z_1^2 = \mu^2 (\dot{z}_2 - \dot{z}_1), \qquad \ddot{z}_2 + z_2 - \frac{1}{2}\mu z_2^2 = \mu^2 (\dot{z}_1 - \dot{z}_2). \tag{29}$$

We use *second-order averaging* on equation (29) for small μ (see Rand, 1994). We set

$$z_i = a_i \cos \varphi_i, \quad \dot{z}_i = -a_i \sin \varphi_i, \quad i = 1, 2. \tag{30}$$

Substitution of (30) into (29) and using variation of parameters gives

$$a_i = -\mu G_i \sin \varphi_i, \quad \varphi_i = 1 - \mu \frac{1}{a_i} G_i \cos \varphi_i, \quad i = 1, 2 \tag{31}$$

where $G_i = \frac{1}{2} z_i^2 + \mu (\dot{z}_j - \dot{z}_i)$, $i = 1, 2$, $j = 2, 1$. Second-order averaging involves a near identity transformation from (a_i, φ_i) to $(\bar{a}_i, \bar{\varphi}_i)$:

$$a_i = \bar{a}_i + \mu\, w_{1i}(\bar{a}_i, \bar{\varphi}_i) + \mu^2 v_{1i}(\bar{a}_i, \bar{\varphi}_i) + O(\mu^3)$$

$$\varphi_i = \bar{\varphi}_i + \mu\, w_{2i}(\bar{a}_i, \bar{\varphi}_i) + \mu^2 v_{2i}(\bar{a}_i, \bar{\varphi}_i) + O(\mu^3) \tag{32}$$

where the generating functions w_{ij} and v_{ij} are chosen to simplify the resulting equations on $\bar{a}_i$ and $\bar{\varphi}_i$ as much as possible. This process results in the following *slow flow*, where we have dropped the bars on a_i and φ_i for convenience and where we have defined

$$\psi = \varphi_2 - \varphi_1 \tag{33}$$

$$\dot{a}_1 = \frac{1}{2}\mu^2 [\, -a_1 + a_2 \cos\psi \,] \tag{34a}$$

$$\dot{a}_2 = \frac{1}{2}\mu^2 [\, -a_2 + a_1 \cos\psi \,] \tag{34b}$$

$$\dot{\psi} = \frac{1}{2}\mu^2 \left[\frac{5}{24}(a_1^2 - a_2^2) - \left[\frac{a_1}{a_2} + \frac{a_2}{a_1} \right] \sin\psi \right]. \tag{34c}$$

Equations (34) are defined on $a_1 - a_2 - \psi$ phase space: $\mathbb{R}^+ \times \mathbb{R}^+ \times S$. Note that $a_1 = a_2$ is an invariant plane L on which the slow flow (34) takes the form

$$\dot{a} = \frac{1}{2}\mu^2 [\, -1 + \cos\psi \,]\, a\,, \quad \dot{\psi} = -\mu^2 \sin\psi \tag{35}$$

where $a = a_1 = a_2$. From (35.2), we see that $\psi = 0$ and $\psi = \pi$ are invariant lines in the plane L. From (35.1), it further follows that the line $\psi = 0$ is composed of equilibria. The flow (35) may be integrated in closed form by writing

$$\frac{da}{d\psi} = -a \frac{\cos\psi - 1}{2 \sin\psi} \tag{36}$$

which has the general solution

$$a = \frac{c}{\sqrt{1 + \cos\psi}} \tag{37}$$

where c is an arbitrary constant (see Figure 9a).

The stability of the equilibrium $a_1 = a_2 = a_0$, $\psi = 0$ may be obtained by computing the eigenvalues of the linear variational matrix:

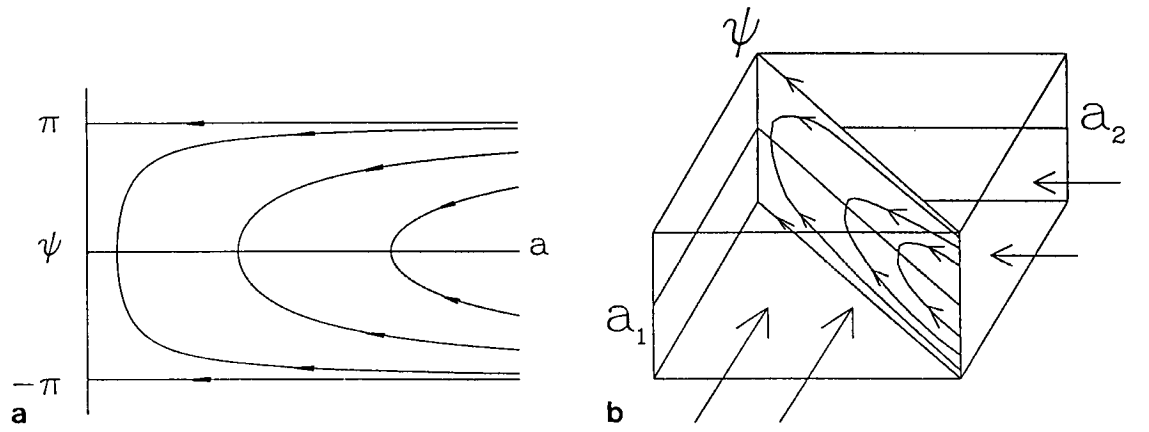

Figure 9. Panel a is the slow-flow (35) on the invariant plane L of equations (34). Panel b is the setting for equations (34) is the $a_1 - a_2 - \psi$ phase space. The top-surface $\psi = \pi$ is identified with the bottom-surface $\psi = -\pi$. The invariant plane L of 9a is shown. The vector field on the planes a_1 = constant and a_2 = constant point into the region as shown.

$$\begin{bmatrix} -1 & 1 & 0 \\ 1 & -1 & 0 \\ \frac{5}{12}a_0 & \frac{5}{12}a_0 & -2 \end{bmatrix} \tag{38}$$

which turn out to be –2, –2, and 0. The eigenvectors corresponding to eigenvalue –2 span a plane perpendicular to the line of equilibria, whereas the eigenvector corresponding to 0 lies along the line of equilibria. Each of these equilibria is therefore attractive, the zero eigenvalue representing the fact that the equilibria are not isolated. Moreover, (34a) shows that $\dot{a}_1 < 0$ for $a_1 > a_2$, so that the vector field is pointing inward on the surface a_1 = constant between the plane $a_2 = 0$ and the plane $a_1 = a_2$, and therefore no motions can escape to infinity across that surface (see Figure 9b). Similarly, (34b) shows that $\dot{a}_2 < 0$ for $a_2 > a_1$, so that no motions can escape to infinity across a_2 = constant between the plane $a_1 = 0$ and the plane $a_1 = a_2$. Because the only equilibria of equations (34) are the line of equilibria $a_1 = a_2$, $\psi = 0$, which lie in plane L, and because no motions can escape to infinity, we are not surprised to find that every motion approaches some equilibrium on this line. See Figure 10, which displays the results of numerical integration of equations (34) projected onto the $a_1 = a_2$ plane.

There remains the question of which equilibrium point a given initial condition will approach. Note that although the local S manifold of an equilibrium on the line $a_1 = a_2$, $\psi = 0$ is two dimensional (being a plane through the equilibrium point and perpendicular to the line of equilibria), a three-dimensional set of orbits must approach each equilibrium point (to account for all initial conditions in the three-dimensional phase space). Figure 11 shows the results of numerical integration of equations (34) for the initial conditions $a_2(0) = 5$ and $\psi(0) = 3$ and for $a_1(0)$ between 0.1 and 10. The vertical axis shows the associated asymptotic value of $a_1 = a_2$. These results are typical of the behavior of the slow flow (34) and illustrate the phenomenon seen in Figure 8 for equations (1). The location of the final periodic orbit (represented by the amplitude $a_1 = a_2$ in the slow flow) depends in an oscillatory fashion on the initial condition. Although the initial conditions of a motion that is destined to be captured may lie far from the interior of the separatrices (where the perturbation study is valid), all captured motions must eventually enter this region, at which point they will experience the phenomena characterized by Figure 11.

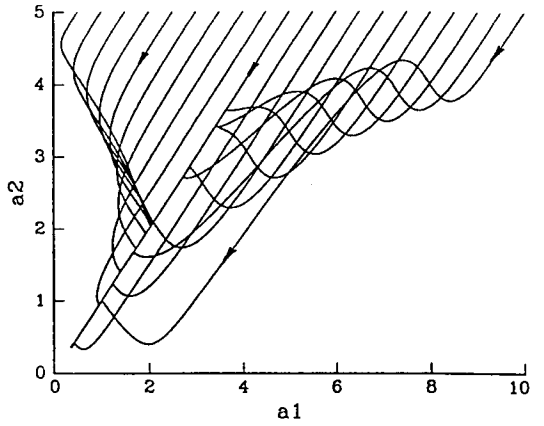

Figure 10. Numerical integration of the slow-flow equations (34) projected onto the $a_1 - a_2$ plane. All trajectories correspond to the initial conditions $\psi(0) = 3$, $a_2(0) = 5$. The initial condition $a_1(0)$ was varied as shown. All motions asymptotically approach the line of equilibria $a_1 = a_2$, $\psi = 0$. The relationship between $a_1(0)$ and the final value of a_1 is displayed in Figure 11.

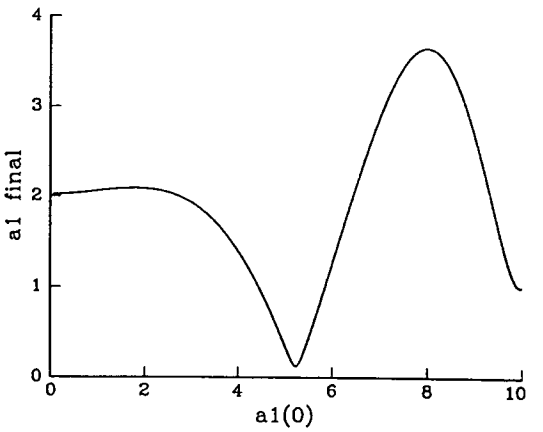

Figure 11. The relationship between $a_1(0)$ and the final value of a_1 of Figure 10 as obtained by numerical integration. Note the qualitative similarity to Figure 8.

SUMMARY AND CONCLUSIONS

We have investigated the dynamics of the coupled system of homoclinic oscillators (1), especially with regard to the question of which initial conditions become captured. In addition to presenting numerical descriptions of the capture region C_ε, we have been able to characterize this set in the special cases of (i) small ε and (ii) special initial conditions in which one oscillator is initially at rest at its stable equilibrium. In the latter case, we used perturbations to generate an approximation for the S manifold of an equilibrium that consists of the center of one oscillator and the saddle of the other.

We found that every motion that is captured approaches some periodic orbit lying in the invariant plane $P, x_1 = x_2$. The question of which initial conditions lead to which periodic orbit was investigated by numerically integrating the system (1) as well as by studying the dynamics of a slow flow based on perturbing the system about the stable equilibria of both uncoupled oscillators.

This work is a first step toward understanding the dynamics of coupled homoclinic oscillators. For example, we would like to better understand the four-dimensional shape of the capture region C_ε and the reasons for its having this shape. Moreover, we are interested in the dynamics of similar systems having other types of coupling—for example, coupling involving the displacements x_i.

APPENDIX

Relation to a System of Coupled Pendulums

In this appendix, we show how equations 1 are related to the equations of motion of two coupled pendulums. Let each of the pendulums be driven by a constant torque of magnitude A, and let the pendulums be coupled by a viscous damper. Then

$$\ddot{\varphi}_1 + \sin \varphi_1 = A + k\,(\dot{\varphi}_2 - \dot{\varphi}_1), \quad \ddot{\varphi}_2 + \sin \varphi_2 = A + k\,(\dot{\varphi}_1 - \dot{\varphi}_2) \tag{A1}$$

where φ_1 and φ_2 are the angular displacements of the pendulums.

Now set

$$\varphi_i = x_i + B \tag{A2}$$

where B is a constant to be chosen appropriately. Substitution of (A2) into (A1) gives

$$\ddot{x}_1 + \sin\,(x_1 + B) = A + k\,(\dot{x}_2 - \dot{x}_1), \quad \ddot{x}_2 + \sin\,(x_2 + B) = A + k\,(\dot{x}_1 - \dot{x}_2) \tag{A3}$$

which gives

$$\ddot{x}_1 + \sin x_1 \cos B + \cos x_1 \sin B = A + k\,(\dot{x}_2 - \dot{x}_1) \tag{A4}$$

and a similar equation on x_2. Taylor expanding the trig terms gives the approximate equation:

$$\ddot{x}_1 + x_1 \cos B + \left(1 - \frac{1}{2}x_1^2\right) \sin B = A + k\,(\dot{x}_2 - \dot{x}_1). \tag{A5}$$

We choose $\sin B = A$ to move the origin to an equilibrium point:

$$\ddot{x}_1 + x_1 \cos B - \frac{1}{2}x_1^2 \sin B = k\,(\dot{x}_2 - \dot{x}_1). \tag{A6}$$

Equation (A6) and the similar equation on x_2 may be cast into the form of equations (1) by taking $B = \frac{3}{4}\pi$, which gives $\sin B = -\cos B = \frac{1}{\sqrt{2}}$, and stretching time so that $\tau = \frac{t}{2^{1/4}}$. This choice of B corresponds to taking the torque $A = \sin B = \frac{1}{\sqrt{2}}$. Also, the quantity ε in equations (1) corresponds to $\varepsilon = 2^{1/4}k$.

REFERENCES

Kauderer, H., 1958, *Nichtlineare Mechanik*, Springer, Berlin.

Magnus, W. and Winkler, S., 1966, *Hill's Equation*, Wiley, New York.

Quinn, D. D. and Rand, R. H., 1995, "A perturbation approach to resonant capture," in *Stability, Vibration and Control of Structures*, A. Guran and D. Inman, eds., Prentice-Hall, Englewood Cliffs, NJ.

Quinn, D., Rand, R., and Bridge, J., 1995, "The dynamics of resonant capture," *Nonlinear Dynamics*.

Rand, R. H., 1994, *Topics in Nonlinear Dynamics With Computer Algebra*, Gordon & Breach, Langhorne, PA.

Rand, R. H. and Armbruster, D., 1987, *Perturbation Methods, Bifurcation Theory and Computer Algebra*, Springer, New York.

Rand, R. H. and Holmes, P. J., 1980, "Bifurcation of periodic motions in two weakly coupled van der Pol oscillators," *International Journal of Non-Linear Mechanics* **15**, 387-399.

Rand, R. H., Kinsey, R. J., and Mingori, D. L., 1992, "Dynamics of spinup through resonance," *International Journal of Non-Linear Mechanics* **27**, 489-502.

Rosenberg, R. M., 1966, "On nonlinear vibrations of systems with many degrees of freedom," in *Advances in Applied Mechanics*, Academic Press, New York, 155-242.

Stoker, J. J., 1950, *Nonlinear Vibrations in Mechanical and Electrical Systems*, Wiley, New York.

Vakakis, A. F., 1994, "Exponentially small splittings of manifolds in a rapidly forced duffing system," *Journal of Sound and Vibration* **170**, 119-129.